ELSEVIER

Journal of Alloys and Compounds 434–435 (2007) 164–166

Journal of ALLOYS AND COMPOUNDS

www.elsevier.com/locate/jallcom

Formation of Cu–Hf–Ti bulk metallic glasses

I.A. Figueroa *, H.A. Davies, I. Todd

Department of Engineering Materials, University of Sheffield, Sheffield S1 3JD, UK

Available online 2 October 2006

Abstract

Alloys of composition $Cu_{55}Hf_{45-x}Ti_x$ with $5 \leq x \leq 45$ at.% and $Cu_{65}Hf_{35-x}Ti_x$ with $5 \leq x \leq 35$ at.% have been investigated. Samples were chill block melt spun to ribbon and produced as cylindrical rods by suction casting into a stepped copper die. All alloys investigated in both series were fully vitrified when melt spun to ribbon of thickness ~25 μm. The compositions $x = 20$ and 25 within the $Cu_{55}Hf_{45-x}Ti_x$ series and $x = 15$ and 20 within the $Cu_{65}Hf_{35-x}Ti_x$ series were found to be the best glass formers, with no crystalline phases detected by XRD for 3 and 4 mm diameter sections, respectively. The composition ranges of highest GFA also had the highest reduced glass temperatures for each of the ranges studied.

Keywords: Metallic glasses; Rapid-solidification; X-ray diffraction; Thermal analysis

1. Introduction

It was demonstrated in 1989 that some alloys based on metals other than Pd could be vitrified in section thicknesses of several mm [1]. Since then, a still increasing number of ternary, quaternary, and higher-order bulk glass-forming alloys have been reported by Inoue et al. [1–3]. In 1993, a family of Zr–Ti–Cu–Ni–Be glasses, with significantly lower critical cooling rates, down to 1 K/s, and supercooled liquid regions up to 135 K were reported [4]. Of these alloys, $Zr_{41.2}Ti_{13.8}Cu_{12.5}Ni_{10}Be_{22.5}$ and $Zr_{46.7}Ti_{8.3}Cu_{7.5}Ni_{10}Be_{27.5}$ had the highest glass forming ability (GFA). Recently, high strength Cu-based bulk glassy alloys were formed in the Cu–Hf–Ti system by the copper mould casting and melt clamp forging methods [5], the substitution of Hf by Ti in the $Cu_{100-x}Hf_x$ system was shown to increase the GFA, so that bulk metallic glasses could be produced in diameters up to 5 mm. However, there is less information available for glassy phases containing more than 50 at.% Cu. This paper presents and discusses the results of a study of glass formation for two series of compositions, $Cu_{55}Hf_{45-x}Ti_x$ and $Cu_{65}Hf_{35-x}Ti_x$.

2. Experimental

Alloy ingots of nominal compositions $Cu_{55}Hf_{45-x}Ti_x$ ($x = 5$, 10, 15, 20, 25, 30, 35 and 40 at.%) and $Cu_{65}Hf_{35-x}Ti_x$ ($x = 5$, 10, 15, 20, 25 and 30 at.%) were prepared by arc melting mixtures of Hf (crystal bar), Cu (sheet) and Ti (rod) having purities of 99.5, 99.99 and 99.8 at.%, respectively. The arc melting was performed in a Ti-gettered high purity argon atmosphere. Each ingot was re-melted at least four times in the arc melter in order to obtain good chemical homogeneity. Ribbon samples of mean thicknesses ~25 μm and width ~2 mm were prepared by melt spinning in a controlled Ar atmosphere. Copper die suction casting was employed to produce rods with a stepped profile having diameters decreasing from 4 to 3 to 2 mm, each with a total length of 50 mm. The phase constitutions of the rods were studied by X-ray diffraction (XRD). The thermal stability, defined by the glass transition temperature (T_g) and the crystallization temperature (T_x), was studied by differential scanning calorimetry (DSC) at a heating rate of 20 K/min. The solidus temperature (T_m) and liquidus temperatures (T_l) were determined by differential thermal analysis (DTA) at a heating rate of 20 K/min. Thermal characterization was performed using melt spun ribbons.

3. Results

Due to the small thickness and the good glass forming ability, all ribbons had an amorphous structure, with high metallic lustre and high bend ductility. The stepped rod samples had good surface quality with few obvious casting defects; an example is shown in Fig. 1.

3.1. $Cu_{55}Hf_{45-x}Ti_x$

Table 1 summarises the results obtained by XRD for all melt-spun ribbon and cast rod samples for this alloys series. While the melt-spun ribbons showed a fully amorphous structure in this composition range, for the bulk samples, the maximum diameter showing a nominally fully amorphous structure was 3 mm for

* Corresponding author. Tel.: +44 114 2225941; fax: +44 114 2225943.
E-mail address: i.a.figueroa@sheffield.ac.uk (I.A. Figueroa).

0925-8388/$ – see front matter © 2006 Elsevier B.V. All rights reserved.
doi:10.1016/j.jallcom.2006.08.181

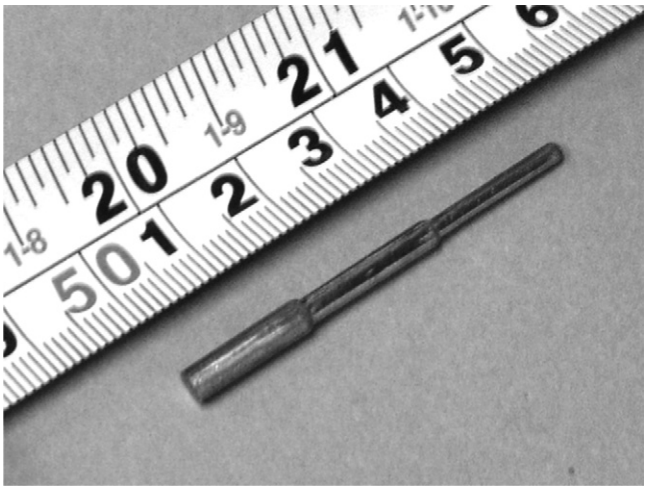

Fig. 1. Suction cast 2, 3 and 4 stepped rod of the $Cu_{65}Hf_{15}Ti_{20}$ alloy.

$x = 20$ and 25, while the 4 mm diameter sections showed significant crystallinity for these compositions. The compositions with $x = 15$ and 30 showed a fully amorphous structure up to 2 mm diameter. Fig. 2 shows the XRD patterns for transverse cross sections of the 3 mm diameter cast rods of the $Cu_{55}Hf_{25}Ti_{20}$ and $Cu_{55}Hf_{20}Ti_{25}$ alloys. Fig. 3 shows that T_g and T_x both decrease progressively with increasing Ti content while T_m and T_l decrease to minimum values at $x \approx 25$ and then increase up to $x = 45$. The quotient T_g/T_l, defined as the reduced glass temperature T_{rg}, increases from 0.56 at $x = 5$ to a maximum of 0.62 at $x \sim 20$, then decreases down to 0.55 for $x = 40$ (Fig. 4a).

3.2. $Cu_{65}Hf_{35-x}Ti_x$

A fully amorphous phase was observed for all the melt-spun ribbons in the composition range studied ($5 \leq x \leq 30$). Bulk rod samples showed a fully glassy structure up to 4 mm diameter for

Table 1
XRD structural results for melt-spun ribbons and for 2, 3 and 4 mm diameter rods, where Am and Cr indicate an amorphous and a crystalline structure, respectively

Composition	Structure at			
	Ribbon	2 mm	3 mm	4 mm
$Cu_{55}Hf_{45-x}$ Ti_x				
$Cu_{55}Hf_{40}Ti_5$	Am	Cr	Cr	Cr
$Cu_{55}Hf_{35}Ti_{10}$	Am	Cr	Cr	Cr
$Cu_{55}Hf_{30}Ti_{15}$	Am	Am	Cr	Cr
$Cu_{55}Hf_{25}Ti_{20}$	Am	Am	Am	Cr
$Cu_{55}Hf_{20}Ti_{25}$	Am	Am	Am	Cr
$Cu_{55}Hf_{15}Ti_{30}$	Am	Am	Cr	Cr
$Cu_{55}Hf_{10}Ti_{35}$	Am	Cr	Cr	Cr
$Cu_{55}Hf_5Ti_{40}$	Am	Cr	Cr	Cr
$Cu_{65}Hf_{35-x}$ Ti_x				
$Cu_{65}Hf_{30}Ti_5$	Am	Am	Cr	Cr
$Cu_{65}Hf_{25}Ti_{10}$	Am	Cr	Cr	Cr
$Cu_{65}Hf_{20}Ti_{15}$	Am	Am	Am	Am
$Cu_{65}Hf_{15}Ti_{20}$	Am	Am	Am	Am
$Cu_{65}Hf_{10}Ti_{25}$	Am	Cr	Cr	Cr
$Cu_{65}Hf_5Ti_{30}$	Am	Cr	Cr	Cr

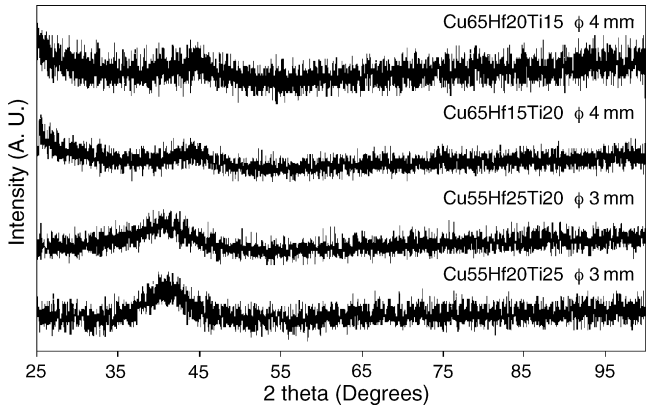

Fig. 2. XRD patterns of cast $Cu_{65}Hf_{35-x}Ti_x$ ($x = 15$ and 20) and $Cu_{55}Hf_{45-x}Ti_x$ ($x = 20$ and 25) alloy rods with diameters of 4 and 3 mm, respectively.

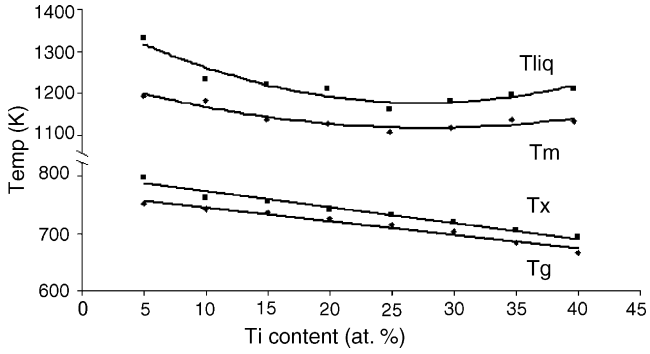

Fig. 3. Plot of T_g, T_x, T_m and T_l for the $Cu_{55}Hf_{45-x}Ti_x$ alloy series.

both $x = 15$ and 20. Interestingly the $x = 5$ alloy showed a fully amorphous structure for the 2 mm diameter section, while the rods for all the remaining composition were partly or fully crystalline (Table 1). Fig. 2 shows the XRD patterns for the transverse cross section of the 4 mm thick cast rods of the $Cu_{65}Hf_{20}Ti_{15}$ and $Cu_{65}Hf_{15}Ti_{20}$ alloys. Fig. 5 shows that both T_g and T_x decreased progressively with increasing Ti content up to $x = 25$ and then

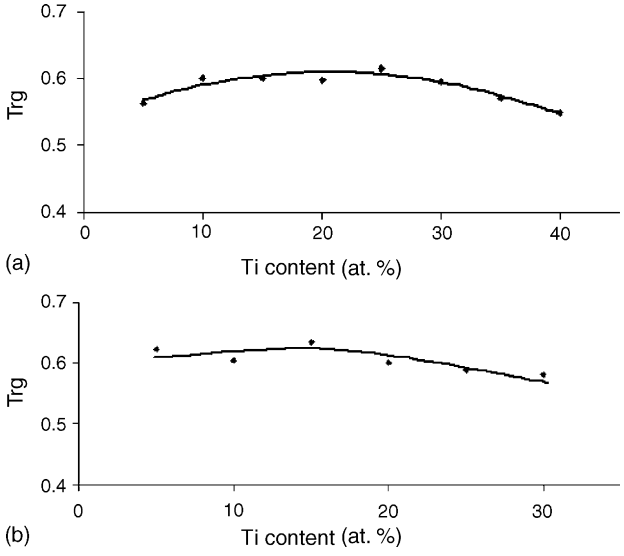

Fig. 4. Plot of T_{rg} for: (a) $Cu_{55}Hf_{45-x}Ti_x$ and (b) $Cu_{65}Hf_{35-x}Ti_x$ alloy series.

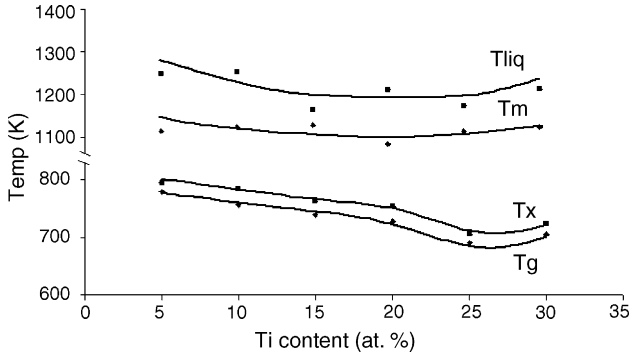

Fig. 5. Plot of T_g, T_x, T_m and T_l for $Cu_{65}Hf_{35-x}Ti_x$ alloy series.

appeared to increase for higher Ti. This corresponded to a change in the crystallisation mode from a single peak to two or three stages; this change in crystallisation behaviour was also seen in the $Cu_{55}Hf_{45-x}Ti_x$ alloy series. T_m and T_l appear to decrease with increasing Ti to minimum values at Ti contents corresponding to $x = 15$–20. The values of T_{rg} are consistently higher than those for the 55 at.% Cu series, with a maximum of ~0.64 for the $x = 15$ alloy (Fig. 4b).

4. Discussion

Increasing the Ti content generally decreased T_g and T_x for both compositional series, consistent with the lower melting temperature and cohesive energy for Ti, in comparison with Hf, although there is evidence for a slight reversal of the trend for the $Cu_{65}Hf_5Ti_{25}$ alloy. On the other hand, the higher Cu series had consistently higher T_g and T_x, which is the opposite of expectation on the basis of simple cohesive energy considerations. The larger maximum T_{rg} for the $Cu_{65}Hf_{35-x}Ti_x$ series than for the $Cu_{55}Hf_{45-x}Ti_x$ series is reflected in its higher experimentally observed GFA for the rod samples [6]. There does not appear to be a clear correlation between the experimental GFA, measured by the critical diameter of fully glassy rod, and the parameter ΔT_x ($=T_x - T_g$), as the Ti content is varied, in either series, and this has also been concluded for other alloy series in this system [5]. Clearly, it is possible to increase T_{rg} by decreasing T_l. This can be achieved by adding further solute atoms of various diameters to the Cu–Hf–Ti alloys. This makes use of the "confusion principle" that can frustrate the tendency of the liquid phase to crystallise by stabilizing it thermodynamically relative to the crystalline phases [7]. The effects of fourth element additions on the GFA of the Cu–Hf–Ti system is highly pertinent.

Inoue et al. [5] have reported DSC and DTA data for Cu–Ti–Hf alloys that were acquired at 40 and 10 K/min, respectively. They reported that the maximum fully glassy rod diameter was 4 mm for the two compositions, $Cu_{60}Hf_{20}Ti_{20}$ and $Cu_{60}Hf_{25}Ti_{15}$. Although, T_{rg} reported here for the alloys of highest GFA are smaller than those reported by Inoue et al. [5], it was still possible to produce fully amorphous rods of diameter 4 mm. This apparent inconsistency can be accounted for on the basis of the different heating rates analysed and different criteria for defining T_g in the two studies.

5. Conclusions

Fully glassy rods with diameters up to 4 mm have been produced for the $x = 15$ and 20 alloys in the 65 at.% Cu series and up to 3 mm for the $x = 20$ and 25 alloys in the 55 at.% Cu series. The composition dependence of the GFA's is consistent with the trends in T_{rg}. The results reported here are in general accord with those obtained by Inoue et al. [5] and by Stewart et al. [8] for $Cu_{60}Hf_{40-x}Ti_x$, for which the GFA also decreased with increasing Ti substitution for Hf.

Acknowledgements

IAF is grateful for the financial support of the Mexican Council of Science and Technology (Conacyt). Valuable technical support provided by Mr. P. Hawksworth is also acknowleged.

References

[1] A. Inoue, T. Zhang, T. Masumoto, Mater. Trans. JIM 30 (1989) 965.
[2] A. Inoue, T. Zhang, T. Masumoto, Mater. Trans. JIM 31 (1990) 177.
[3] A. Inoue, Mater. Trans. JIM 36 (1995) 866.
[4] A. Peker, W.L. Johnson, Appl. Phys. Lett. 63 (1993) 2342.
[5] A. Inoue, et al., J. Non-Cryst. Solids 304 (2002) 200.
[6] H.A. Davies, Phys. Chem. Glasses 17 (1976) 159.
[7] A.L. Greer, Nature 366 (1993).
[8] P. Stewart, P.A. Carroll, H.A. Davies, H. Jones, unpublished data.